EARTH SCIENCES
RESEARCH JOURNAL

Eart Sci. Res. J. Vol. 18, No. 2 (December, 2014): 173 - 179

GIS

UNIVERSIDAD NACIONAL DE COLOMBIA
SEDE BOGOTÁ
FACULTAD DE CIENCIAS
DEPARTAMENTO DE GEOCIENCIAS
RESEARCH GROUP IN GEOPHYSICS

Spatial distribution of sediment pollution in the Khajeh Kory River using Kriging and GIS

Maryam Zare Khosh Eghbal
Department of Mathematics and Science, Astara Branch, Islamic Azad University, Astara, Iran
E-mail: m.zare@iau-astara.ac.ir

ABSTRACT

The aim of this research was to study of sediment pollution conditions in the river bed of Khajeh Kory, which passes from the southern border of the Caspian Sea in Astara City. To determine the pollution of river bed sediment along the route, from the river source in the heights to estuary in the Caspian sea, sampling was conducted at 10 stations. Afterward, each sample was divided into two groups based on size (>63 µm and <63 µm). The concentration of heavy metals Cu, Cd, Co, Zn, Pb, Ni, Fe, and Mn in each group was measured using ICP-OES. In the next stage, the enrichment of samples was determined by normalization with aluminum. The data were then interpolated using the Kriging method and various models (including spherical, circular, exponential, Gaussian) were fitted to the data, and the best method was selected using the Cross Validation method. Using the obtained enrichment outcomes, an information layer was produced for each element in the GIS environment utilizing the Kriging method. The layers were aggregated and the compiled layer was classified into 4 layers again. Using this method, the length of the river from its source to the sea estuary was characterized based on the contamination of heavy metals, and contaminated and unpolluted areas in river sediments could be observed. The source of this pollution, either natural or manmade, was revealed through this method.

Key words: Sediment pollution, Khajeh Kory River, Kriging, GIS

RESUMEN

El objeto de esta investigación fue estudiar las condiciones de contaminación sedimentaria en el lecho del río Khajeh Kory, que se extiende desde el borde sur del Mar Caspio en la ciudad de Astara. Para determinar la contaminación del lecho sedimentario, se recolectaron muestras en 10 estaciones establecidas entre la fuente del río en sus partes altas hasta los estuarios en el Mar Caspio. Después, cada muestra fue dividida en dos grupos de acuerdo con el tamaño (>63 µm and <63 µm). La concentración de metales pesados Cu, Cd, Co, Zn, Pb, Ni, Fe y Mn en cada grupo se midió con la técnica ICP-OES. En la siguiente etapa, se determinó el enriquecimiento de las muestras por la normalización con aluminio. Los datos se interpolaron luego con el método Kriging y varios modelos (incluidos el esférico, el circular, el exponencial, el gaussiano) se ajustaron a la información y se seleccionó el mejor método a través de la Validación Cruzada. Con los resultados obtenidos del enriquecimiento se produjo una capa de información para cada elemento en el ambiente GIS a través del método Kriging. Las capas fueron agregadas y la compilación de estas se clasificó nuevamente en otras cuatro capas. De esta forma se caracterizó el río a lo largo, desde su nacimiento hasta el estuario marino, con base en la contaminación de metales pesados y se pudo distinguir entre las zonas contaminadas y las áreas limpias en sedimentos. Las fuentes de esta contaminación, sean naturales o humanas, también se identificaron con este método.

Palabras clave: Sedimentos contaminados; río Khajeh Kory; Kriging; GIS

Record

Manuscript received: 19/07/2014
Accepted for publication: 16/09/2014

ISSN 1794-6190 e-ISSN 2339-3459
http://dx.doi.org/10.15446/esrj.v18n2.44491

Introduction:

Rivers are an essential aquatic ecosystems, and rivers are polluted by various contaminants (Bednarova et al., 2013). One class of most important pollutants is heavy metals. Heavy metals are ecologically impactful because they experience high resistance in the environment, accumulate in natural resources, and ultimately enter the food cycle (Varol & *Şen*, 2012). River sediments are the ultimate destination of these metals (Maanan et al, 2013). Geochemistry-based methods have been considered appropriate in determining the contaminated condition of these deposits (Meybeck, Horowitz, & Grosbois, 2004). The Guilan province is especially notable for contamination as various rivers directly or indirectly pour into the Caspian Sea. Within this province a number of urban areas, urban sewage, domestic wastewater, and industrial sewage play important roles in the contamination of rivers (Gheshlagh, Ziarati, & Bidgoli, 2013). Domestic wastewaters are poured into special attraction wells within each residential unit in rural areas. However, various agricultural fertilizers and pesticides are common in this area because of rice cultivation and the use of other agricultural lands. These materials enter the river along with surface drainage and cause pollution. Additionally, the land may also contain high levels of heavy metals due to special lithology and geology, naturally causing contamination without human interference (Salati & Moore, 2010). The Khajeh Kory River is located in the western part of Guilan and passes along forest, agricultural, and residential areas upstream and crosses Astara downstream to pour into the Caspian Sea. The aim of this study is to investigate contamination conditions in this river from different sections from its source (areas without agricultural lands and human sewage) to river estuaries at the sea (areas that receive urban and rural sewage, as well as agricultural land surface drainage).

One problem in measuring the contamination of an area or river involves the limited sampling possible within an area or along the river length; to overcome this problem, interpolation methods should be used. Interpolation analysis is in line with the spatial characteristics of methods that are common in spatial statistics studies (Xie et al., 2011) and is based on the principle that points that are closer in space are also likely to be more similar to each other than to points that are further apart. There are various spatial interpolation algorithms that are based on geostatistical and geometric methods. Recently, the use of GIS software has been utilized in the spatial modeling arena and a variety of studies have been conducted in interpolation analyses for zoning contamination sites (Mcgrath, Zhang, &Carton, 2004). Validation of these methods requires precision and various factors are recommended. In the present study, geographic information system (GIS) and standard Kriging methods have been used to prepare interpolation maps to examine heavy metal contamination in the Khajeh Kory River.

Materials and Methods:

In the studied area, the sediments of the Khajeh Kory River covers a watershed area of 10233 hectare, located in the Guilan province, which ranges between 38° 20′ 45″ and 38° 26′ 45″ latitude and 48° 42′ 22″ and 48° 52′ 28″ longitude. This watershed is covered with forest (63.12%), agricultural and garden lands(12.71%) and 2.47% rural and urban areas (Figure 1).

Geologically, the basin is covered with structures from the Mesozoic and Cenozoic ages. The main part of basin (44.5%) is composed of pevet units from the Paleocene age with Alternation of Tuff ,Tuffereous Sandstone with Pyroxin.

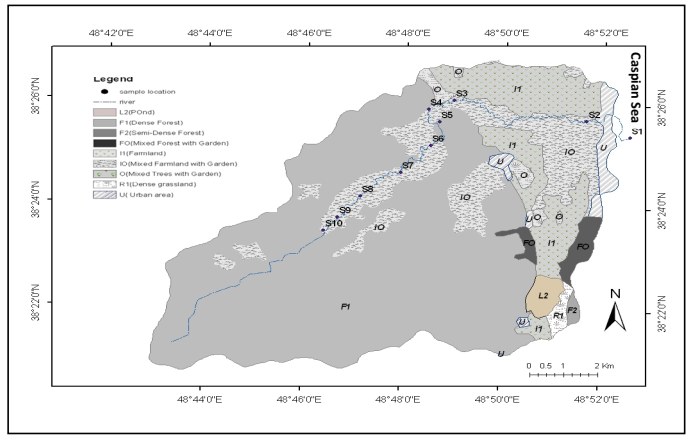

Figure 1: Land use map in the Khajeh Kory watershed area.

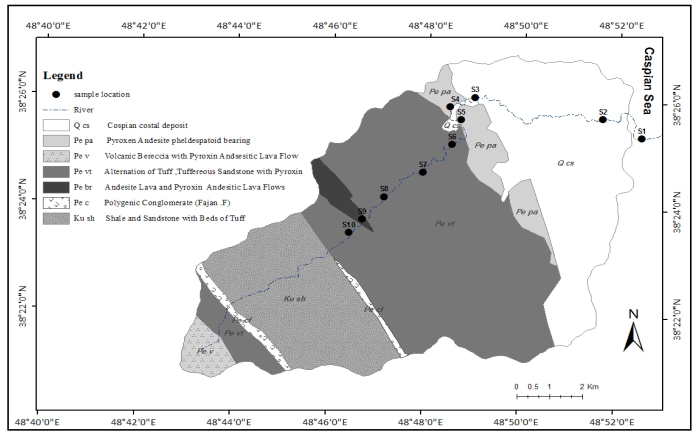

Figure 2: Geological map of the Khajeh Kory watershed area.

This Special lithology can cause an increase in the measurements of elements in the area and is given special attention. Qcs units encompassing the quaternary age cover 27.33% of the total area and constitute the second most prevalent the type of sediment in the Caspian Sea coastal plain (Figure 2).

Figure 2 is a geological map of the area and was prepared using Arc GIS 10 software and georeferencing a 1:100000 map of Astara geology. Sampling stations were selected to cover a range of various sites depending on the land use and type of lithology in the area. The pattern of sampling and the condition of each area are represented in Figure 1. After sampling stations were determined (Singh, Mohan, Singh, & Malik, 2005), trapped sediments were sampled from each station (Horowitz, 2009). Sediments were dried at ambient air temperature in laboratory conditions. Dried sediments were powdered and divided by size into two groups (>63 *μm* (muddy part) and <63 *μm)*, and each group was subjected to ICP-OES (Inductively Coupled Plasma Optical Emission Spectrometry) to determine the concentration of elements, including Cu, Cd, Co, Zn, Pb, Ni, Fe, and Mn. ICP-OES uses plasma to prepare qualitative and quantitative analyses of elements. In our analysis, the argon gas was ionized using a magnetic field (radio frequency of 27-40 MH) and the temperature was ~10,000 K. The sample was infused into the plasma using a nebulizer, and the high temperature sample was converted to ions and diffused through the sediments. The rate of diffusion was measured by the apparatus. After determining the elemental concentrations, a method must be applied for quantitative measurement of elemental contamination. One such method uses aluminum as a standard in normalizing sediments samples (Choi, Kim, Hong, & Kim, 2013). Aluminum is present in high amounts as a result of erosion in stones and its presence is sediment is not affected by human activities. Conversely, aluminum has variable solubility, can chemically react in soil, and migrates after being deposited in sediment. Normalization based on aluminum

content occurs in two stages. First, the concentrations of each element in a sample are divided by the concentration of aluminum, and the sample with the least variation is selected as the reference sample. Second, the amount of pollution is obtained by the ratio of a given element to aluminum in the sample and compared to an inner reference sample using the following formula:

$$EF = [X / Al] \text{ sample} / [X / Al] \text{ ref}$$

In the following method, the descriptive statistics of analysis and geostatistics will be used to fit the best data to an enrichment model. Finally, an enrichment map is prepared for each element, and after merging the elements, a cumulative map of pollution weight in river foot can be produced.

Statistical Methods:

1. Descriptive statistics of data: To investigate the distribution of element enrichment and to summarize the statistical information of contamination, concentration of each element In ppm was evaluated for maximum, minimum, mean, standard deviation and variance using SPSS software.

2. Geostatistical analyses: Geostatistics is capable of modeling uncertain temporal and spatial phenomena. Basically, geostatistics estimates each unknown value as a random number within a known probable distribution across an understudied space (Dao, Morrison, Kiely, & Zhang, 2013). Before using the data, the normality of data needs to be determined (Kroulík, Mimra, Kumhála, & Prošek, 2006.) and both Kolmogorov and Smirnov tests are used to test the distribution of data with a reliability of 5% and 1%, respectively. After determining the normality of the data, geostatistics is used to correlate information of a point to the information of that area on a map. The Kriging method of geostatistics was used to interpolate, zonate, and forecast the probability of data correlation.

3. Analyzing variograms: After checking the normality of the data, Kriging measurements were implemented in calculating a variogram. A variogram is a function that measures the variability of spatial data; it is extremely important in spatial data correlation and is the base of geostatistics (Kaushik, Kansal, Kumari, & Kaushik, 2009; Maanan, et al., 2013). Dividing a variogram in two, we can obtain easily understood semivariograms, which is the practical use in geostatistical methods. Semivariograms are represented by $\gamma(h)$ and can be calculated according to the following relation:

$$\gamma(h) = \frac{1}{2n}\sum_{i=1}^{n}[Z_i(x) - Z_i(x+h)]^2$$

In this equation, n is the number of sample couples per distance, h; Zi (x) is the value of variance in i point; and $Z_i(x+h)$ indicates the value of variance in a point that is h distance from point i. Increasing h, the value of semivariogram is increased to a certain distance and then fixed at a threshold level, sill. The distance between samples at which variable values have minimal effect on each other and the value of semivariogram does not significantly differ is called the range of influence. The value of the semivariogram when h=0 is called the Nugget effect (Figure 3) (Liu, Wu, & Xu, 2006).

The Nugget effect usually results from errors in data sampling, measurement and, analysis. The less the Nugget effect, the less the estimation error will be. Variogram modeling is an iterative process.

In all geostatistical interpolation methods, including Kriging, unknown values are estimated using the following equation:

$$Z^*(x) = \sum_{i=1}^{n}\lambda_i Z(x_i)$$

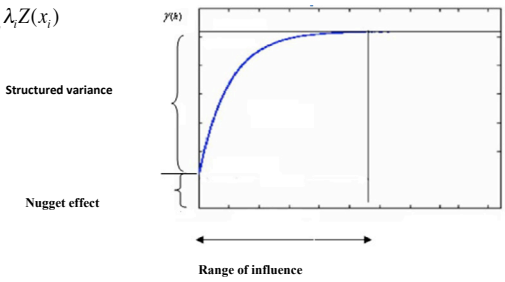

Figure 3: Schematic image of the variogram and its parameters.

In this equation, Z(Xi) indicates the value of observable Z variable at Xi, λi indicates the weight of a given ratio to Z variable at Xi, and n is the number of observations. After drawing an experimental variogram, four models (including circular, spherical, exponential, and Gaussian) were fitted for each data set.

4. Assessment methods, criterion, and validation models:

In the present study, the methods used to control and validate parameters used in the estimation will be assessed as a method of cross-validation. This method requires deleting samples and re-estimating them using the Kriging method, followed by using other samplings and fitted models in an experimental variogram (angulo-martínez, lópez-vicente, vicente-serrano, & beguería, 2009). Following the subtraction of real and estimated values, the estimations are statistically evaluated (Castrignanò, Giugliarini, Risaliti, & Martinelli, 2000). In the present research, validation models and estimations were evaluated by calculating the root mean square (RMS) criteria and the standard root mean square (SRMS) values using the following formulas:

$$RMS = \sqrt{\frac{1}{n}\sum_{i=1}^{n}(z_{i,act} - z_{i.est})^2} \qquad SRMS = \sqrt{\frac{1}{n}\sum_{i=1}^{n}\frac{(z_{i,act} - z_{i,est})^2}{S^2}} = \frac{RMS}{S}$$

In these formula, n is the number of points $z_{i,act}$ indicates the value of i at a known point, $z_{i,est}$ is the estimation of i known point, and S indicates error variation. The best estimation should have a minimal RMS, and SRMS should approximate 1. If SRMS equals 1, it means that RMS is equal to S (Angulo-Martínez, et al., 2009). Generally, the smaller the RMS, the more precise the method will be. Theoretically, if this criterion equals zero, the method precision is one hundred percent and the estimated value of a quantity is equal to its real value.

Discussions and Results:

Table 1 details the changes in the elemental concentrations in the sediments from the Khajeh Kory River. These results demonstrate that the heavy metal concentrations were mainly found in fine-grain deposits (Fang, Jiang, Wang, & Xie, 2010; Kaushik, et al., 2009). Additionally, the highest concentrations of iron were found in station s10; the maximum concentrations of manganese, cobalt, and cadmium were found in s3; the maximum concentration of nickel was found in s9; the maximum concentration of lead was found in s1; and the maximum concentration of zinc was found in s7. In regard to sampling station placements by geological units and land use, station 1 (s1) reveals high values of lead, which result from urban life and petrol use in that area. The abundance of iron in s10 comes from natural, geological sources as there are no contamination factors from agriculture, urban and rural sewage, or industry. Conversely, constitutive rocks in this area are mainly composed of pyroxene, which contain iron and magnesium components. Three stations, including s9, s8, and s7, have similar compositions. Therefore, the noted frequency of zinc in s7 is of non-geological origins and likely originates from the neighboring Besat residential suburb, which utilizes gable roofs that are composed of galvanized zinc. This zinc can decompose due to rainfall and enter surface water, resulting in higher concentrations in sediments. Abundance of manganese, cobalt, and cadmium in s3 among agricultural lands is likely a result of chemical fertilizers and pesticides used in rice fields, which are common in the area.

Table 1: Concentrations of selected elements of sample sediments from sampling stations.

Sample	Fe	7.14	Cd	Co	Cu	Ni	Pb	Zn
S1 f	4.86	3.76	0.27	25	63	50	117	2116
S1 c	4.64	5.37	0.26	23	36	47	18	88
S2 f	4.48	0.79	0.27	21	59	54	65	407
S2 c	5.16	0.63	0.25	24	42	45	20	86
S3 f	5.59	7.14	0.4	30	75	53	35	114
S3 c	5.14	3.76	0.27	22	57	41	19	89
S4 f	5.03	5.37	0.28	22	59	51	34	630
S4 c	4.56	0.79	0.25	22	37	47	25	92
S5 f	5.37	0.63	0.28	25	66	55	35	1920
S5 c	6.35	7.14	0.26	27	44	53	39	100
S6 f	5.36	3.76	0.27	27	61	59	40	723
S6 c	6.03	5.37	0.26	27	51	58	29	104
S7 f	4.95	0.79	0.27	24	57	53	37	4529
S7 c	5.94	0.63	0.24	26	48	57	32	119
S8 f	4.85	7.14	0.8	27	64	60	51	201
S8 c	6.42	3.76	0.25	26	47	61	21	100
S9 f	3.76	5.37	0.28	17	60	44	100	2696
S9 c	5.75	0.79	0.23	23	40	56	19	96
S10 f	5.93	0.63	0.26	26	69	45	28	345
S10 c	7.14	7.14	0.25	30	47	60	48	113
Max	7.14	3.76	0.8	30	75	61	117	4529
Min	3.76	5.37	0.23	17	36	41	18	86
Average	5.37	0.79	0.3	24.7	54.1	52.45	40.6	733.4
Standard deviation	0.79	0.63	0.12	3.11	11.1	6	26.27	1182
Variance	0.63	7.14	0.02	9.69	123.15	36.05	689.94	1396988.9

f * indicates fine-grain (smaller than 63 micron) and c indicated coarse-grain (greater than 63 μm).

The enrichment factor values and use of normality method by Al in various stations is described in Table 2. Enrichment factors are used in this analysis instead of absolute elemental concentrations because of differences in densities between elements. For instance some elements, including iron and manganese, are more common in the crust and are measured in percent, whereas other elements are less abundant and are measured in ppm. Using enrichment as an index without dimension is effective and efficient because it allows for different analyses to be conducted without needing to consider the differences between the amounts of individual elements. These results indicate that the pollution is mostly in fine-grain sediment (Rodríguez, Ruiz, Alonso-Azcárate, & Rincón, 2009; Seshan, Natesan, & Deepthi, 2010). Additionally, S3 stations contained the highest amounts of Mn, Co, and Cu. The level of Zn enrichment was found to be 30 times higher in this area. After the river crosses Astara city, where it begins to pour into the Caspian sea, there is an 18.73-enrichment of zinc, which demonstrates that there is a relationship with residential and agricultural areas (Bai et al., 2011).

Table 2: The results of element enrichment factors in sediment samples.

Sample	X	Y	Fe	Mn	Cd	Co	Cu	Ni	Pb	Zn
S1 f	313741	4255467	0.61	0.76	0.7	0.67	0.97	0.72	3.79	15.92
S1 c	313741	4255467	0.89	0.9	1.03	0.95	0.85	1.03	0.89	1.01
S2 f	313277	4255522	0.56	1.28	0.69	0.56	0.9	0.77	2.08	3.03
S2 c	313277	4255522	1	1	1	1	1	1	1	1
S3 f	309388	4256292	0.7	2.22	1.03	0.8	1.15	0.76	1.13	0.85
S3 c	309388	4256292	0.9	0.82	0.97	0.82	1.22	0.82	0.85	0.93
S4 f	308955	4255522	0.62	0.58	0.72	0.59	0.9	0.72	1.09	4.68
S4 c	308955	4255522	0.87	0.81	0.99	0.91	0.87	1.03	1.23	1.06
S5 f	308627	4255966	0.6	0.53	0.65	0.6	0.91	0.71	1.01	12.91
S5 c	308627	4255966	1.22	0.99	1.03	1.12	1.04	1.17	1.93	1.15
S6 f	307798	4253708	0.65	0.85	0.67	0.7	0.91	0.82	1.25	5.25

S6 c	307798	4253708	0.89	0.76	0.79	0.85	0.92	0.98	1.1	0.92
S7 f	308689	4254667	0.63	1.01	0.7	0.65	0.89	0.77	1.21	34.35
S7 c	308689	4254667	0.98	0.77	0.81	0.92	0.97	1.08	1.36	1.17
S8 f	306606	4252861	0.58	1.24	1.99	0.7	0.95	0.83	1.58	1.45
S8 c	306606	4252861	1.1	0.81	0.89	0.96	0.99	1.2	0.93	1.03
S9 f	305939	4252099	0.51	0.77	0.79	0.5	1.01	0.69	3.53	22.1
S9 c	305939	4252099	1.27	0.93	1.05	1.09	1.08	1.42	1.08	1.27
S10 f	305527	4251633	0.6	0.62	0.54	0.57	0.86	0.52	0.73	2.1
S10 c	305527	4251633	1.22	0.88	0.88	1.1	0.99	1.18	2.12	1.16

To process geostatistics, the normality of the data must first be evaluated, and the Kolmogorov-Smirnov test is used to distribute normal data (Dao, et al., 2013). The results of this test are illustrated in Table 3. This test indicated that all parameters have a normal distribution at a 0.05 level.

Table 3: The results of Kolmogorov – smirnov in enrichment rate of river sediments.

		Fe	Mn	Cd	Co	Cu	Ni	Pb	Zn
N		10	10	10	10	10	10	10	10
Normal Parameters a, b	Mean	0.61	0.99	0.85	0.63	0.94	0.73	1.74	10.26
	Std. Deviation	0.05	0.51	0.42	0.09	0.08	0.09	1.07	11.06
Most Extreme Differences	Absolute	0.16	0.21	0.36	0.14	0.26	0.22	0.28	0.28
	Positive	0.15	0.21	0.36	0.14	0.26	0.13	0.28	0.28
	Negative	-0.16	-0.18	-0.23	-0.10	-0.16	-0.22	-0.18	-0.20
Kolmogorov-Smirnov Z		0.52	0.65	1.125	0.45	0.819	0.684	0.873	0.87
Asymp. Sig. (2-tailed)		0.95	0.79	0.16	0.99	0.51	0.74	0.43	0.44

After calculating and drawing experimental variograms, four models (including spherical, circular, exponential, Gaussian) were fitted using experimental semi-variograms for each data set; the parameters for each one are displayed in Table 4.

Table 4: Variogram parameters for each of the elements.

Parameter	model	Nugget Effect	Partial sill	Nugget/ partial sill	RMS	SRMS
Fe	Circular	0.00151	0.00135	1.1156	0.05047	1.022
	Spherical	0.00150	0.00137	1.0950	0.05028	1.017
	Exponential	0.00146	0.00153	0.9517	0.05119	1.023
	Gaussian	0.00167	0.00127	1.3165	0.05061	1.031
Mn	Circular	0	0.36795	0	0.5347	0.8304
	Spherical	0	0.36795	0	0.5399	0.8376
	Exponential	0.01416	0.36795	0.0385	0.554	0.8569
	Gaussian	0.00500	0.36795	0.0136	0.5352	0.8459
Cd	Circular	0	0.24437	0	0.4221	0.8868
	Spherical	0	0.24816	0	0.4274	0.8901
	Exponential	0	0.29234	0	0.4552	0.9356
	Gaussian	0.00028	0.27828	0	0.4142	0.9015
Co	Circular	0	0.00867	0	0.08893	0.9204
	Spherical	0	0.00867	0	0.08956	0.9236
	Exponential	0	0.03115	0	0.09237	0.9404
	Gaussian	8.98E-06	0.00898	0	0.08999	0.9269
Cu	Circular	0	0.01064	0	0.09753	0.8729
	Spherical	0.00262	0.00936	0.2794	0.09714	0.9326
	Exponential	0	0.01237	0	0.09722	0.8957
	Gaussian	1.09E-05	0.01090	0.0010	0.09552	0.8687

Ni	Circular	0.00167	0.00554	0.3016	0.08104	0.9855
	Spherical	0.00179	0.00546	0.3282	0.0809	0.9866
	Exponential	0	0.00726	0	0.08408	1.005
	Gaussian	0.00290	0.00439	0.66013	0.0807	0.9896
Pb	Circular	0.74358	0.59072	1.2588	1.158	1.096
	Spherical	0.73107	0.55505	1.3171	1.155	1.098
	Exponential	0.82256	0.34810	2.3630	1.154	1.07
	Gaussian	0.65856	0.94277	0.6985	0.4142	0.9015
Zn	Circular	0	296.44	0	15.22	1.09
	Spherical	0	267.18	0	14.97	1.046
	Exponential	0	239.63	0	13.75	0.922
	Gaussian	15.83	243.24	0.0651	15.17	1.063

As indicated in Table 4, the Nugget effects of Zn, Co, and Cd elements for three models (including spherical, circular, and exponential) equals zero. Low ratios of Nugget/partial sill represent the spatial coherence of variables and the lesser this ratio, the greater the spatial coherence of the data will be (Angulo-Martínez, et al., 2009). The smallest ratios of this value were observed for cadmium, cobalt, and zinc in the three models. It is not possible to comment on the best data fit model because of the low Nugget/sill for Zn, Cd, and Co in the three different models; more calculations are required. Cross-validation was conducted to validate the data using standard root mean square (SRMS) value and root mean square (RMS) values. The calculated SRMS and RMS values fitted from various models on different semi-variograms are given in Table 4.

The variogram with the smallest RMS indicates the best model for the sample. The best models for each element were as follows: the exponential model for Zn; the Gaussian model for Pb, Cu, Cd, and Ni; the spherical model for Fe; and the circular model for Co and Mn. In regards to the SRMS values, the use of Kriging in spatial changes of selected data indicated that optimal estimation had been performed.

Preparing the map of contamination zoning:

As described using the Kriging method, the smallest RMS establishes the criterion for selecting the best model. With this consideration, the best model was obtained for enrichment values of each elements. High precision estimation of the parameters in this and other studies (Angulo-Martínez, et al., 2009; Bai, et al., 2011; Bednarova, et al., 2013; Castrignanò, et al., 2000; Dao, et al., 2013) indicates that geostatistical methods are appropriate for studying spatial changes in data, using the necessary calculations when there is a lack of data.

To obtain the best Kriging models in GIS, which are used to determine and interpret pollution in river sediments, raster layer were first generated for each element based on the best selected model during the Kriging application stage (Table 4). Then, all raster layers were compiled, the resulting map was grouped into four classes, and the pollution zoning map was used to interpret pollution deposits in the Khajeh Kory river.

Figure 4: Map of the superficial sediments accumulating in river pollution.

To decrease uneven weighing effects by various factors, the raster map for each parameter was divided into four classes. These four class maps were collected, and the cumulative map was divided into four classes. The final map indicates that much of the river length contains high accumulations of contamination and that upstream parts of the river basin have been mainly formed from Pyroxene deposits from the Besat suburb, which contains the most pollution and largely depends on the igneous lithology of area (Figure 4). As heavy metals exclusively demonstrate different contamination levels along the route and because cumulative contamination relies on multiple factors that are unique to each heavy metal, this implies different responses in the soil contamination of an element.

Conclusion:

The conducted studies revealed that geochemical characteristics and river contamination differ at various points. The reason for this difference is based on the concentration of population centers, the way of life within these centers, land uses, and geology. Urban population primarily concentrates in the eastern part of the drainage basin and decreases from east to west. The results demonstrate that elemental concentrations, excluding iron, increase as the river approaches the sea. Iron concentration are higher upstream, as in station s10, despite the lack of contaminating agricultural land and residential areas; this is due to the ferruginous lithology of the area. Additionally, the Zn concentrations do not follow a clear pattern as the concentration fluctuates among different basin points and is at high concentrations after crossing all the basins and prior to entering to the sea. Data from fine-grain samples from each station (s1f, s2f, s3f, s4f, s5f, s6f, s7f, s8f, s9f, s10f) were normalized, using aluminum, to determine enrichment. Pollution can concentrate in fine-grain texture, and the data from this texture indicates area contamination. Then, using the Kriging method, the enrichment factor of the samples was converted to a map in an GIS environment. To validate this map, RMS factors were calculated and the most validated model was determined to fit each sample. Next the data were converted to a surface map based on the best interpolation model as determined using Kriging method. The obtained maps for each element were then converted to raster layer and these layers were collected, which may provide evidence of pollution. The results of classification indicate that much of the river length experiences low values of contamination. In addition, major parts of the river route contain low values of contaminants. The rest of the river route contains medium to high contamination. The highest amounts of contamination were observed between where the rivers exits the city and enters the sea, as well as in the areas crossing rice fields. In addition, in the heights with igneous lithology, high levels of contamination were observed around station s7 next to the Besat residential suburb. As the river passes among pyroxene masses in the heights, the pollution is observed to be andesitic. This work highlights that the high rate of contamination in the Khajeh Kory drainage basin is from either natural or manmade sources. In the heights, the residential areas do not have considerable concentrations of heavy metals. Additionally, there are no rice fields that can

cause contamination, and the dominant coverage is natural rainforest. Therefore, the existence of contamination in the heights is definitely related to the geology of the area. Abundance of iron in river sediment after passing through the mass confirms its role in increasing elemental concentrations. The main reason for manmade contamination in the basin, excepting residential areas, are fertilizers and pesticides used in rice fields and the use of highly enriched lead, petrol and worn tires of transportation vehicles in urban areas. Additionally, in urban areas, the main cause of contamination is domestic and urban sewage pouring into the river and the accumulation of waste on its banks.

Recommendations:

Contamination is one of the most important factors threatening the Khajeh Kory River ecosystem. As noted previously, wastes and effluents are considered to be the main sources of contamination. Drainage water from agricultural lands contains high percentages of chemical fertilizers and materials that pour into the river. It is recommended that rivers should be managed to prevent solid waste accumulation and promote recycling and that the concentration of heavy metals in sewage feeding into the river should be monitored. Additionally, sampling time intervals should be reduced and conducted in different seasons of the year to better and precisely analyze contamination in future research.

References:

Angulo-Martínez, M., López-Vicente, M., Vicente-Serrano, S. M., & Beguería, S. (2009). Mapping rainfall erosivity at a regional scale: a comparison of interpolation methods in the Ebro Basin (NE Spai).

Bai, J., Xiao, R., Cui, B., Zhang, K., Wang, Q., Liu, X., et al. (2011). Assessment of heavy metal pollution in wetland soils from the young and old reclaimed regions in the Pearl River Estuary, South China. Environmental Pollution, 159(3), 817-824.

Bednarova, Z., Kuta, J., Kohut, L., Machat, J., Klanova, J., Holoubek, I., et al. (2013). Spatial patterns and temporal changes of heavy metal distributions in river sediments in a region with multiple pollution sources. Journal of Soils and Sediments, 1-13.

Castrignanò, A., Giugliarini, L., Risaliti, R., & Martinelli, N. (2000). Study of spatial relationships among some soil physico-chemical properties of a field in central Italy using multivariate geostatistics. Geoderma, 97(1), 39-60.

Choi, K. Y., Kim, S. H., Hong, G. H., & Kim, C. J. (2013). Metal contamination and potential toxicity of sediment from lock gate port in South Korea.

Dao, L., Morrison, L., Kiely, G., & Zhang, C. (2013). Spatial distribution of potentially bioavailable metals in surface soils of a contaminated sports ground in Galway, Ireland. Environmental geochemistry and health, 1-12.

Fang, F., Jiang, B., Wang, H., & Xie, H.-f. (2010). Particle size distribution and health risk assessment of heavy metals in surface dust of Wuhu urban area. Geographical Research, 29(7), 1193-1202.

Gheshlagh, F. S.-N., Ziarati, P., & Bidgoli, S. A. (2013). Seasonal Fluctuation of Heavy Metal and Nitrate Pollution in ground water of Farmlands in Talesh, Gilan, Iran.

Horowitz, A. J. (2009). Monitoring suspended sediments and associated chemical constituents in urban environments: lessons from the city of Atlanta, Georgia, USA Water Quality Monitoring Program. Journal of Soils and Sediments, 9(4), 342-363.

Kaushik, A., Kansal, A., Kumari, S., & Kaushik, C. (2009). Heavy metal contamination of river Yamuna, Haryana, India: Assessment by metal enrichment factor of the sediments. Journal of hazardous materials, 164(1), 265-270.

Kroulík, M., Mimra, M., Kumhála, F., & Prošek, V. (2006). Mapping spatial variability of soil properties and yield by using geostatic method. Research in Agricultural Engineering, 1, 17-24.

Liu, X., Wu, J., & Xu, J. (2006). Characterizing the risk assessment of heavy metals and sampling uncertainty analysis in paddy field by geostatistics and GIS. Environmental Pollution, 141(2), 257-264.

Maanan, M., Landesman, C., Maanan, M., Zourarah, B., Fattal, P., & Sahabi, M. (2013). Evaluation of the anthropogenic influx of metal and metalloid contaminants into the Moulay Bousselham lagoon, Morocco, using chemometric methods coupled to geographical information systems. Environmental Science and Pollution Research, 1-13.

McGrath, D., Zhang, C., & Carton, O. T. (2004). Geostatistical analyses and hazard assessment on soil lead in Silvermines area, Ireland. Environmental Pollution, 127(2), 239-248.

Meybeck, M., Horowitz, A. J., & Grosbois, C. (2004). The geochemistry of Seine River Basin particulate matter: distribution of an integrated metal pollution index. Science of the total environment, 328(1), 219-236.

Rodríguez, L., Ruiz, E., Alonso-Azcárate, J., & Rincón, J. (2009). Heavy metal distribution and chemical speciation in tailings and soils around a Pb–Zn mine in Spain. Journal of Environmental Management, 90(2), 1106-1116.

Salati, S., & Moore, F. (2010). Assessment of heavy metal concentration in the Khoshk River water and sediment, Shiraz, Southwest Iran. Environmental monitoring and assessment, 164(1-4), 677-689.

Seshan, B., Natesan, U., & Deepthi, K. (2010). Geochemical and statistical approach for evaluation of heavy metal pollution in core sediments in southeast coast of India. International Journal of Environmental Science and Technology, 7(2), 291-306.

Singh, K. P., Mohan, D., Singh, V. K., & Malik, A. (2005). Studies on distribution and fractionation of heavy metals in Gomti river sediments—a tributary of the Ganges, India. Journal of hydrology, 312(1), 14-27.

Varol, M., & Şen, B. (2012). Assessment of nutrient and heavy metal contamination in surface water and sediments of the upper Tigris River, Turkey. Catena, 92, 1-10.

Xie, Y., Chen, T.-b., Lei, M., Yang, J., Guo, Q.-j., Song, B., et al. (2011). Spatial distribution of soil heavy metal pollution estimated by different interpolation methods: Accuracy and uncertainty analysis. Chemosphere, 82(3), 468-476.